환상형 공진기와 방사형 도파관 급전구조를 이용한 고효율 평면안테나에 관한 연구

정회원 정 기 혁*, 종신회원 나 극 환*

High Aperture Efficiency Flat Antenna using Annular Ring Resonators and Radial Waveguide Feeder Network

Ki Hyeok Jeong* *Regular Members*, Keuk hwan Ra* *Lifelong Members*

요 약

본 논문에서는 위성을 이용한 디지털 위성방송 시스템에 적용하기 위한 고효율 평면안테나를 설계 및 제작하였다. 전통적인 접시형 안테나에 비하여 높은 개구효율, 용이한 설치 및 미려한 외관 등의 장점을 가지고 있는 평면안테나를 설계하였다. 안테나 소자의 설계에는 마이크로스트립을 이용한 Annular Ring 공진기를 이용하였으며, 방사형 도파관을 이용한 급전구조를 채택하였다. 또한 수신신호를 중간주파 신호로 변환하기 위한 LNB를 안테나의 뒷면에 설치함으로써 전송손실의 최소화를 꾀하였다. 제작된 안테나는 직경 35cm, 이득은 31.8dBi 이며 개구효율은 약 80%이다.

Key Words : Flat Antenna, Koreasat, Annular Ring, LHCP, Microstrip

ABSTRACT

An antenna was designed and manufactured for the DBS receiver system. This antenna is a planar or flat antenna which shows many advantages over the conventional parabolic antenna such as higher aperture efficiency, easier installation and improved aesthetics to name a few. The antenna is a novel design employing microstrip annular ring resonating antenna elements and a radial waveguide feeder network. The LNB(Low Noise Blockdown Converter) is can integrate with the antenna at the back of the radial waveguide. The 35cm diameter antenna works at 31.8dBi minimum gain which implies an aperture efficiency of around 80%.

Ⅰ. Introduction

The successful introduction of the Digital Satellite System(DSS) in 1994 signaled the opening of a new era in digital DBS, in USA. Since then, numerous other private companies as well as governments have followed suit with their own digital DBS systems covering single countries or continents.

The digital DBS system holds significant advantages over the analog system. A single analog channel can now hold over 4 digital channels through the use of digital compression technology(MPEG-2) and time division multiplexing of the different signals. Also, the digital signals provide clearer pictures and CD quality sound. The digital format of

the data also provides for ISDB(Integrated Services Digital Broadcasting) such as HDTV, PC communications, VOD, etc.

In terms of the cost in establishing the broadcast network infrastructure, satellite is cheaper per subscriber as compared to terrestrial broadcasting which must cover wide areas by constructing a multitude of transmitter towers which can cover only around a 100km's radius. Also, simultaneous nation-wide or even multi-national broadcasting is possible with all areas within the footprint capable of receiving the signal which is clear of ghost noise found in terrestrial broadcasting.

Korea has also joined this bandwagon with its own DBS system which began test broadcasting of two KBS channels from the Koreasat satellite in July 1996, and then started SkyLife service with Koreasat 3 in November 2001. Similar to its predecessors, the Koreasat DBS utilizes MPEG-2 compression technology for a various channels using LHCP (Left Hand Circular Polarization)[1].

Ⅱ. Planar Antenna

2.1 Link Budget for Koreasat DBS

Through an extensive link budget analysis based on a receiver locatedat Sinpo which is a North Korean city located on the -3dB EIRP contour of Koreasat, it was determined that a 31.8dB gain antenna with a 1.1dB noise Fig. LNB(Low Noise Blockdown converter) will provide for around 99.9% operation, with a C/N >7dB necessary for noise free picture recovery. The following link budget equation was used in the evaluation.

$$C/N = EIRP - Pathloss + G/T - Lp - K - B \qquad (1)$$

Where, EIRP : Effective Isotropic Radiated Power
Pathloss : Free Space Propagation Loss
G/T : Antenna Gain to System Noise Temperature, which is the Fig. of Merit of an Antenna and LNB
Lp : Rain and Atmospheric Attenuation
K : Boltzmann's constant
B : Receiving Bandwidth

Until now, antennas used for satellite signal reception have mainly been limited to reflector antennas which consist of prime-focus, offset or cassegrain configurations.

For reception of the high powered Ku band signals used in DBS, offset antennas are used. The antenna efficiency is limited to around 75% due mainly to losses incurred by the feedhorn illumination taper as well as irregularities with the reflector surface. The antenna efficiency can expressed as

$$Efficiency = 100 \times \frac{G\lambda^2}{4\pi A} \qquad (2)$$

where G is Antenna Gain and A is Antenna Aperture Area

Therefore a gain of 31.8dB translates to an offset antenna with around 38cm diameter. The increased transponder power and frequency have meant that smaller antennas can be used. This has led to the development of various types of planar antennas utilizing what was previously military radar technology.

2.2 Planar Antenna

Planar or "flat" antennas as they are often referred to as, usually consist of hundreds of resonating antenna elements which are around half wavelength long, or they consist of hundreds of radiating discontinuities in a traveling wave transmission structure.

The signals received from each of the elements are combined using a microwave feeder network and fed to the LNB circuit which amplifies and downconverts the 12GHz signal to the 1GHz IF(Intermediate Frequency) signal for input into the satellite receiver. Examples of previous planar antenna structures are listed in table 1.

As compared to reflector antennas, the advantages to be gained from planar antennas are higher efficiency, smaller profile, light weight, easy installation, better performance in adverse weather and improved aesthetics.

The DBS antenna must meet goals that are quite contradictory. It must possess professional perfor-

689

Table 1. Previous planar antenna structures.

Description	Drawing	Radiation Element	Feeding Network
One point feed Circular Patch		Patch	Microstrip
Two point feed Rectangular Patch		Patch	Microstrip
Aperture Slot		Slot	Triplate
Circular Patch and Slot		Patch	Triplate
Radial Line Slot		Slot	Waveguide
Radial Line Helical		Discontinuity	Waveguide
Rectangular Waveguide Slot		Discontinuity	Waveguide
Crank type		Discontinuity	Microstrip

mance to satisfy the high performance requirements for satellite communications and at the same time it must be of low cost for the consumer market and this must be comparable to the cost for the offset reflector antenna.

Taking all performance, cost, as well as manufacturing considerations into account. We decided on a novel antenna consisting of an annular ring microstrip antenna and a feeder network consisting of a radial waveguide.

The annular ring microstrip antenna, which is resonating in the TM$_{11}$ mode show good performance among the resonating antenna elements in terms of bandwidth. In comparison to the feeder losses associated with the microstrip line(-4dB/m) or the triplate(-2dB/m), the radial waveguide shows almost no loss(-0.1dB/m) due to the absence of dielectric loss as well as radiation loss[2,3].

The LNB is integrated with the antenna and attached at the metal back plate. This reduces loss during signal transfer from antenna to LNB and improves overall gain as well as noise of the receiver system. Furthermore, novel ideas were incorporated into the antenna structure in order to improve antenna manufacturability and lower cost.

III. Antenna Element Design

3.1 Basic Annular Ring Antenna

Firstly, we need to investigate the properties of the basic annular microstrip antenna which produces linearly polarized radiation fields.
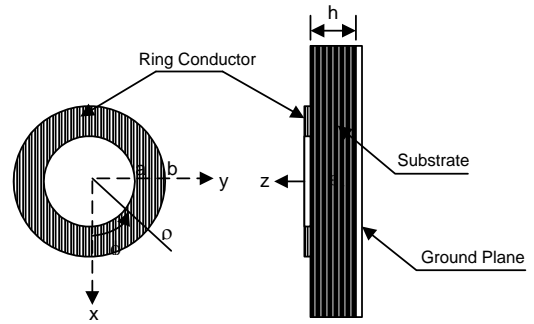
Fig. 1. Annular ring microstrip antenna element geometry

The annular antenna geometry, comprising a ring-shaped strip conductor on one side of a dielectric substrate backed by a ground plane, is shown in Fig. 1[4]. The solutions for the fields can be obtained by using the cavity model in which the annulus is surrounded by magnetic walls. Since h ≪ λ$_o$, there is no variation of the electric field in the z direction and the fields can be assumed to be TM. For TM$_{nm}$ modes, the electric and magnetic field distributions for a ring resonator in the cylindrical coordinate system(ρ,ϕ,z) are given by

$$E_z = E_o[J_n(K\rho)Y_n'(Ka) - J_n'(Ka)Y_n(k\rho)]\cos n\Phi \quad (3)$$

$$H = \frac{j\omega\ni}{k^2\rho} \cdot \frac{\partial E_z}{\partial \Phi} \quad (4)$$

$$H_\Phi = \frac{-j\omega\ni}{k^2} \cdot \frac{\partial E_z}{\partial \rho} \quad (5)$$

Where J_n and Y_n are Bessel functions of the first and second kind, and of order n, respectively. The prime sign signifies derivatives of the Bessel functions, ε is the permittivity of the dielectric and $k = 2\pi\sqrt{\varepsilon_r}/\lambda_o$ (where ε_r is the relative permitivity and λ_o is the free space wavelength). The integer n denotes the azimuth mode number, and the integer m denotes the variation of the fields across the

width of the ring. The surface currents on the annulus may then be found from $K_\Phi = -H_\rho$ and $K_\rho = -H_\Phi$. The radial components of this current must vanish along the edge[5]:

$$K_\rho(\rho = b) = H_\Phi(\rho = b) = 0 \qquad (6)$$

Hence from equations (3), (4) and (6):

$$J_n'(Kb) Y_n'(ka) - J_n'(Ka) Y_n'(kb) = 0 \qquad (7)$$

Then equation (7) is solved for various modes.
An approximate value of k can also be obtained using:

$$k = \frac{2n}{a + b} \qquad (8)$$

This expression gives a reasonably accurate value of k for $n \leq 5$ and $(b-a)/(b+a) \leq 0.35$.
The resonant frequency can be calculated by taking into account the effect of fringing fields, using:

$$f_r = \frac{ck}{2\pi\sqrt{\varepsilon_e}} \qquad (9)$$

where ε_e is the effective dielectric constant for a microstrip line of strip width $W = b - a$. The frequency difference between the theoretical values and experimental results is approximately 3%.

3.2 Circular Polarized Annular Ring

The DBS signals from the KOREASAT are LHCP(left hand circularly polarized). Therefore, the antenna elements must also produce circularly polarized fields.

The basic annular ring linearly polarized antenna can be modified into a singly-fed CP(circularly polarized) antenna element by the addition of two perturbation segments at the edge of the ring. The TM11 dominant mode is separated into two orthogonal modes. When the amount of perturbation segment(ΔS) is adjusted to be the optimum value, the two modes are excited in equal amplitude and 90oout of phase at the center frequency as shown in Fig. 2. This enables the antenna to act as a CP radiator in spite of single feeding[6,7,8,9].
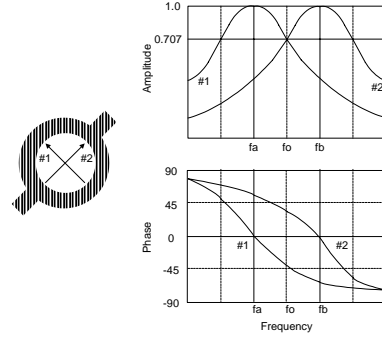
Fig. 2. Conditions required for circular polarization

The equivalent circuit after perturbation is shown as two uncoupled parallel resonant circuits excited by the common voltage source V_o as shown in Fig. 3. The operating condition for circular polarization can be determined by circuit theory from this equivalent circuit.
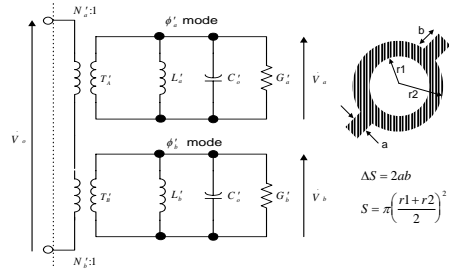
$$\omega_{or} \cong \omega_a \cong \omega_b \qquad N_b' = K \sin(\phi_F + 45^o)$$

$$f_{or} = \frac{1.841 C}{2\pi \bar{a} \sqrt{\varepsilon_r}} \qquad K = \sqrt{2}\sqrt{\frac{\chi_{11}^2}{\chi_{11}^2 - 1}}$$

$$f_o' = f_{or}\left(1 - \frac{1}{2}\frac{\Delta S}{S}\right) \qquad \chi_{11} = 1.841, \ Q_{oa} = Q_{ob} = Q_o$$
$$L_a' = 1/(\omega_a^2 C_o'), \ L_b' = 1/(\omega_b^2 C_o')$$

$$\frac{\Delta f_a'}{f_{or}} = 0.4185\frac{\Delta s}{S}$$
$$\frac{\Delta f_b'}{f_{or}} = -1.4185\frac{\Delta s}{S} \qquad \begin{array}{l} G_a' = \omega_a C_o'/Q_{oa}, \\ G_b' = \omega_b C_o'/Q_{ob} \\ C_o' = \varepsilon S/h \end{array}$$

$$f_a = f_{or} + \Delta f_a', \qquad \phi_F : \text{feed angle}$$
$$f_b = f_{or} + \Delta f_b' \qquad C : \text{light velocity}$$

$$\omega_a = 2\pi f_a, \ \omega_b = 2\pi f_b \qquad \dot{Y}_a = G_a' + j\{\omega C_o' - 1/(\omega L_a')\}$$
$$N' = K\cos(\phi_F + 45^o) \qquad \dot{Y}_b = G_b' + j\{\omega C_o' - 1/(\omega L_b')\}$$

$$\frac{\dot{V}_b}{\dot{V}_a} = \frac{N_b'}{N_a'}\frac{\dot{Y}_a}{\dot{Y}_b} = \frac{N_b'}{N_a'}\left\{\frac{\left(\frac{f_a}{Q_{oa}}\right) + j\left(f - \frac{f_a^2}{f}\right)}{\left(\frac{f_b}{Q_{ob}}\right) + j\left(f - \frac{f_b^2}{f}\right)}\right\}$$

Fig. 3. Equivalent circuit and equations for the CP antenna element

691

$\bar{V}_a$ and $\bar{V}_b$ in the equivalent circuit correspond to the radiation fields of the orthogonal modes $\Phi_a{}'$ and $\Phi_b{}'$ after perturbation. By application of the CP conditions satisfying $|\bar{V}_a/\bar{V}_b| = 1$ and $\arg(\bar{V}_a/\bar{V}_b) = \pm 90$ to the above equations, the following relation is obtained.

$$|\Delta s/S|Q_o = 1/\chi_{11} \tag{10}$$

where $\Delta s/S$, Q_o and χ_{11} correspond to the amount of perturbation, the unloaded Q and the eigen value of the dominant TM_{11} mode, respectively.

Using the above mentioned equations, the following structural dimensions are obtained for our annular ring microstrip antenna element.

a : 1 mm
b : 1.5 mm
r1 : 2.9 mm
r2 : 4.1 mm

The Fig. 4 shows results of moment method full wave analysis for the final design using a commercially available software. Fig. 4 (a) shows the current vectors found on the surface of the microstrip antenna element and (b) shows the far field radiation obtained from this distribution.

(a)

(b)

Fig. 4. Full wave analysis result

IV. Antenna Array Design

The above mentioned elements can now be arrayed on the radial waveguide to construct a planar antenna. The transverse electromagnetic (TEM) mode propagates in the radial waveguide provided the spacing of the two parallel plates is sufficiently small compared with the wavelength. For this reason, the height of the waveguide is chosen to be 7.5mm. The following functions describe the fields within the waveguide.

$$H_\Phi = k_\rho H_1^{(1)}(k_\rho \rho) \tag{11}$$

$$E_Z = \frac{k^2}{j\omega\varepsilon} H_1^{(1)}(k_\rho \rho) \tag{12}$$

$$E_\rho = E_\Phi = H_\rho = H_Z = 0$$
$$k = \omega\sqrt{\mu\varepsilon} \tag{13}$$

Where $H_n^{(1)}$ is the Hankel function of the first kind of order n.

Inside the radial waveguide, as the name implies, a radially outward traveling wave is used to feed the antenna elements. The annular microstrip antenna elements are excited by linear probes which are partially inserted into the radial waveguide through a small hole in the upper metal ground plate. This linear probe is held in place without touching the ground plate by an insulating plastic. A portion of the power being radiated outward in the waveguide is coupled to this probe and radiated out into free space through the resonating antenna element; the remaining power travels on to the next element in the radial direction.

4.1 Design for Uniform Aperture Power Distribution

Due to the angular spread of the power in the radial waveguide, power flow density is tapered at a rate of $1/\sqrt{\rho}$. If the probe length is uniform for all the antenna elements, the aperture radiated power would be tapered even more steeply.

However, for the radial waveguide to work with maximum efficiency, it must have uniform aperture

field distribution in terms of radiated power as well as phase for each of the antenna elements.

In order to compensate for the inherent power flow density taper in the radial waveguide. The length of the coupling probe inserted into the w/g is varied so that coupling increases, in other words probe depth increases with ρ.
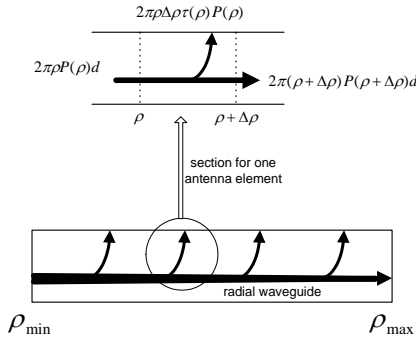

Fig. 5. Power flow within radial waveguide

The energy conservation in the radial line is written as

$$2\pi\rho P(\rho)d - 2\pi(\rho+\Delta\rho)P(\rho+\Delta\rho)d$$
$$= 2\pi\rho\Delta\rho\tau(\rho)P(\rho) \quad (14)$$

where $P(\rho)$ is the power flow density at ρ, $\tau(\rho)$ indicates the ratio of radiation from slot to inner power and d is the height of the guide. Taking the limit of $\Delta\rho\rightarrow0$, we have the next equation:

$$\frac{d}{d\rho}\{\rho P(\rho)\} = -2\alpha(\rho)\rho P(\rho) \quad (15)$$

where $\tau(\rho)/2d$ is defined as the coupling factor $\alpha(\rho)(>0)$, which reflects all the structural parameters. Solving it for $P(\rho)$, we have aperture power distribution $\alpha(\rho)P(\rho)$ as

$$\alpha(\rho)P(\rho) = \frac{\alpha(\rho)\rho_{min}}{\rho}\exp\left\{-2\int_{\rho_{min}}^{\rho}\alpha(\rho)d\rho\right\} \quad (16)$$

In order to realize uniform illuminations, $\alpha(\rho)P(\rho)$ constant is imposed in equation (16) and the coupling factor $\alpha(\rho)$ is given as

$$\alpha(\rho) = \frac{\rho}{K-\rho^2} \quad,\quad K = \frac{\rho_{max}^2 - t\cdot\rho_{min}^2}{1-t} \quad (17)$$

where $t(<1)$ is the power dissipated at the termination.

The following probe lengths where chosen in order to achieve the coupling factor in equation (17) for uniform power illumination.

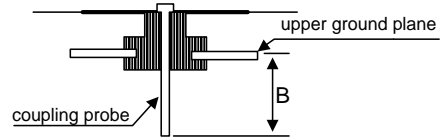| Radial distance from Center	Probe depth B
20 mm	3.75 mm
40 mm	4 mm
60 mm	4.25 mm
80 mm	4.5 mm
100 mm	4.5 mm
120 mm	5.5 mm
140 mm	6.75 mm
160 mm	7.25 mm

Fig. 6. Cross section of antenna element and coupling probe

4.2 Design for Uniform Aperture Field Distribution

Furthermore, in order to achieve uniform aperture phase distribution, the signals radiating off of each of the antenna elements must be of coherent phase. This implies that the elements circularly arrayed at the eight different circumferences must be separated by a radial distance of guide wavelength λg for the radiated power to be equi-phased. Since there is no material filling the waveguide interior other than air, λg is equivalent to the free space wavelength. However, if the antenna elements are separated by the free space wavelength, this gives rise to grating lobes in the radiation pattern.

As shown in Fig. 7, the radial distance was set at 2cm's which is equivalent to a 285 degree phase
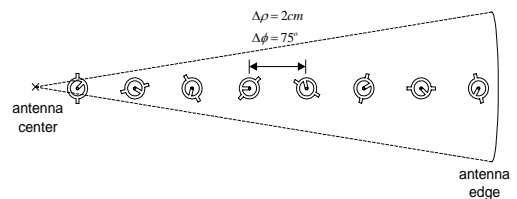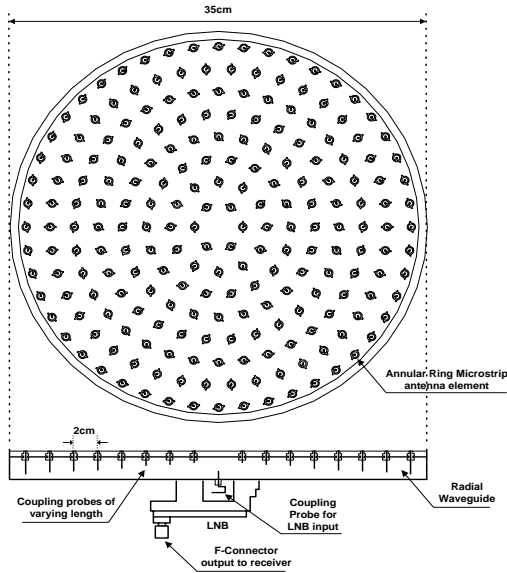

Fig. 7. Antenna layout in the radial direction

693

Fig. 8. Antenna array layout and cross section

Fig. 9. Antenna cross section and signal flow

Fig. 10. Photograph of array pattern

difference. In order to compensate for this phase difference, the antenna elements are rotated clockwise by 75 degree in sequence from the center. The final layout for the arrayed elements is shown in Fig. 8.

Ⅴ. Antenna Structure and Manufacturing Methode

Fig. 9 shows a cross section of our antenna showing the inner workings. The circularly polarized signal from the satellite first penetrates the radome. This is made out of press molded acrylic plastic which must be invisible to the electromagnetic field and also withstand harsh outdoor conditions such as impact as well as wide temperature variations during winter and summer. The signal is then coupled to the resonating elements which are patterned on polyester film by screen printing of silver ink as shown in Fig. 10. This signal then travels down the coupling probe pin into the radial waveguide whose top and bottom ground plates are made of Nickel plated Steel. This brass pin is inserted in the center of each of the 216 antenna elements and it is held in place by an insulating plastic made of poly-propylene. The signal then travels towards the center of the
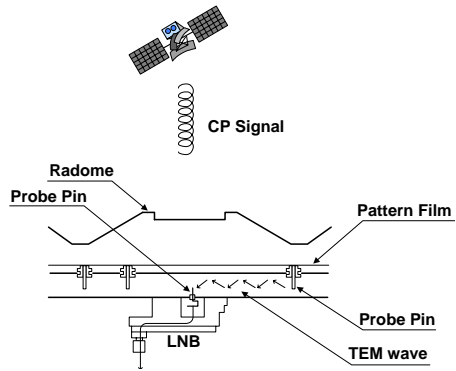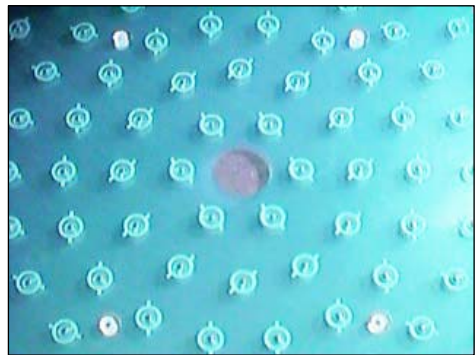
waveguide where it is coupled to another coupling probe which transfers the signal to the input waveguide(WR75) of the LNB.

Ⅵ. Antenna Measurement Results

The antenna farfield radiation pattern was measured at the 11.85 Ghz center frequency using a nearfield scanner. Amplitude and phase measurements made in the nearfield region at a Nyquist sampling distance are Fourier transformed to produce the farfield radiation data.

The resulting 3D plot of the farfield is shown in Fig. 11 and its 2D cross section is shown in Fig. 12. It shows a sharp main lobe with 4.26 degree beamwidth directed towards the broadside. The first sidelobe appears at -13.64 dB and the gain of thisantenna sample is 32.1 dBi. Fig. 13 shows results of reflection measurements measured between 9.85 to 13.85 Ghz. The reflection at 11.85Ghz is -13.6dB.
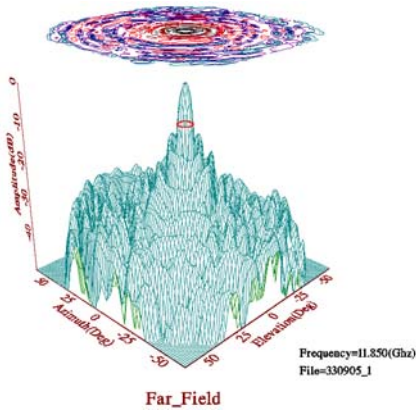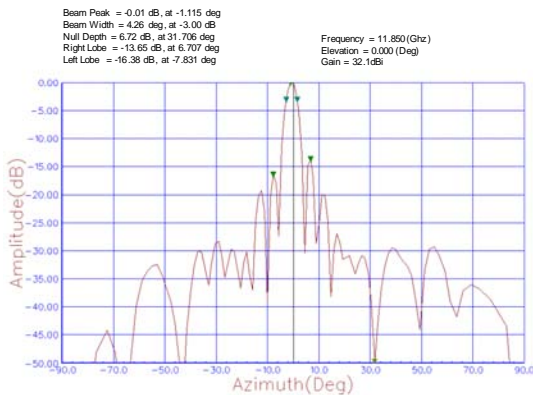
694

Fig. 11. 3D Far-field radiation pattern

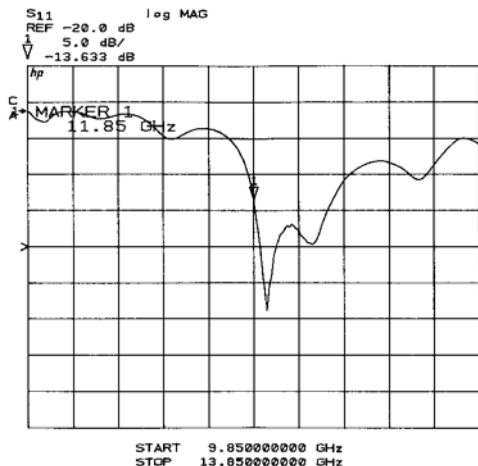**Fig. 12.** Cross Section of 3D radiation pattern

Fig. 13. Reflection measurement of antenna input

Ⅶ. Conclusions

The antenna was carefully designed for its aesthetic appeal so that it could be used indoors near windows with a clear view towards the satellite. Because it has adequate gain margin, it work well even behind thick curtains.

The performance of this antenna is comparable to that of 40cm offset antennas currently on the market. For the next stage in antenna development, our goal is to improve efficiency above 90%, which would reduce diameter from 35cm's now to 30cm's.

Also, there is a growing market for antenna systems with real-time tracking capabilities that can be installed on moving vehicles. Currently, there are mechanical tracking systems but we expect that this will soon be replaced by electronically steered phased array systems.

As more and more satellites fill the skies, in the future, a single planar antenna will receive from multiple satellites. This antenna will support wide bandwidths, multiple polarizations as well as phase steering. But most importantly it must be low cost.

REFERENCES

〔1〕 진재선, 강기조, 이학용, 진형석, 이병제, 김남영, 김종헌, 이종철, "위성방송수신용 이중 원형편파 마이크로스트립 배열안테나", 한국통신학회논문집, Vol.23, No.1, pp.876~879, 2001년 7월.

〔2〕 Wu, Y.S. and F.J. Rosenbaum, "Mode Chart for Mcrostrip Resonators," *IEEE Trans. On Microwave Theory and Tech*., Vol. MTT-21, pp. 487-489, 1973.

〔3〕 Bahl, I.J., S.S. Stuchly and M.A. Stuchly, "A New Microstrip Radiator for Medical Applications," *IEEE Trans. On Microwave Theory and Tech*., Vol. MTT-28, pp. 464-468, 1980.

〔4〕 Kompa, G. and R. Mehran, "Planar Waveguide Model for Calculating Microstrip Components," *Electron. Lett*., Vol. 11, pp. 459-460, 1975.

〔5〕 Carver, K. R., and Mink, J. W., "Microstrip Antenna Technology," *IEEE Trans. On Antennas and Propagation*, Vol. AP-29, pp. 2-24, 1981.

〔6〕 Mink, J.W., "Circular Ring Microstrip Antenna Elements," *IEEE AP-S Int. Symp. Digest 1980*, pp. 605-608.

〔7〕 Kerr, J.L., "Microstrip Polarization Techniques,"

695

Symposium on Antenna Applications, University of Illinois, Sept. 1978.

〔8〕 Richards, Y. F., LO, Y. T., and Simon, P., "Design and Theory of Circularly Polarized Microstrip Antennas," *IEEE AP-S International Symposium Digest*, pp. 117-120, June 1979.

〔9〕 Takahashi, M., Taakada, J., Ando, M. and Goto, N., "Characteristics of Small-Aperture, Single -Layered Radial-Line Slot Antennas," *IEE Proceedings-H*, Vol. 139, pp. 79-83, Feb. 1992.

〔9〕 G. Gonzalez, "*Microwave Transistor Amplifiers Analysis and Design,*" Prentice-Hall, Inc., 1984.

정 기 혁(Ki Hyeok Jeong)   정회원

1990년 2월 광운대학교 전자공학과(학사)

1992년 8월 광운대학교 전자공학과(석사)

2002년 3월~현재 광운대학교 전자공학과 박사과정

1992년 8월~1997.11 대우전자 영상연구소 주임연구원

1997년 12월~2001년 11월 (주)한화/정보통신 무선연구단 선임연구원

2002년 2월~현재 (주)엠티아이 책임연구원

<관심분야> 이동 및 위성통신, 휴대인터넷 시스템

나 극 환(Keuk hwan Ra)   종신회원

1973년 2월 연세대학교 전자공학과(학사)

1977년 2월 연세대학교 전자공학과(석사)

1981년 7월 프랑스 ENSEEIHT 국립종합공과대학 전자공학과(박사)

1987년 1월~1988년 1월 미국 COMSAT연구소 객원연구원

1981년 9월~현재 광운대학교 전자공학과 교수

<관심분야> 마이크로파 공학, 이동 및 위성통신, 레이다